Skin Research and Technology 2017; 23: 354–362
Printed in Singapore · All rights reserved
doi: 10.1111/srt.12342

Published by John Wiley & Sons Ltd
Skin Research and Technology

Automatic facial pore analysis system using multi-scale pore detection

J. Y. Sun[1], S. W. Kim[1], S. H. Lee[1], J. E. Choi[2] and S. J. Ko[1]

[1]Department of Electrical Engineering, Korea University, Seoul, Korea and [2]Department of Dermatology, College of Medicine, Korea University, Seoul, Korea

Background/purpose: As facial pore widening and its treatments have become common concerns in the beauty care field, the necessity for an objective pore-analyzing system has been increased. Conventional apparatuses lack in usability requiring strong light sources and a cumbersome photographing process, and they often yield unsatisfactory analysis results. This study was conducted to develop an image processing technique for automatic facial pore analysis.

Methods: The proposed method detects facial pores using multi-scale detection and optimal scale selection scheme and then extracts pore-related features such as total area, average size, depth, and the number of pores. Facial photographs of 50 subjects were graded by two expert dermatologists, and correlation analyses between the features and clinical grading were conducted. We also compared our analysis result with those of conventional pore-analyzing devices.

Results: The number of large pores and the average pore size were highly correlated with the severity of pore enlargement. In comparison with the conventional devices, the proposed analysis system achieved better performance showing stronger correlation with the clinical grading.

Conclusion: The proposed system is highly accurate and reliable for measuring the severity of skin pore enlargement. It can be suitably used for objective assessment of the pore tightening treatments.

Key words: facial pore – pore widening – noninvasive evaluation – multi-scale pore detection – image processing – Delaunay triangulation

Accepted for publication 23 September 2016

THE TERM 'skin pore' refers to the visible features on the skin surface caused by enlarged openings of pilosebaceous follicles (1, 2). As conspicuous facial pores are becoming common beauty concerns in the cosmetic field, a variety of treatment modalities for reducing the size of facial pores are being developed and launched in the market (3), such as retinoid applications (4), chemical peeling (5), and different kinds of laser therapies (6–8). Accordingly, an objective and quantitative pore analysis system has become necessary to diagnose the severity of pore widening and evaluate the effectiveness of the pore tightening products and treatments.

Some analytic apparatuses such as JANUS Facial Analysis System (JANUS) (PSI Co. Ltd., Gyeonggi, Korea), Robo Skin Analyzer CS 50 (RSA) (Inforward Inc., Tokyo, Japan), and Mobile Smart Scope (MSS) (Moritex Corp., Saitama, Japan) were recently developed for measuring the extent of pore widening. With this equipment, skin images are acquired from built-in cameras, and the analyses are carried out through their own image processing based analysis software. JANUS and RSA always need strong light sources since their performance is significantly affected by the lighting environment. Moreover, patients should wear the light absorbing clothes and attach their faces to the equipment to block out the ambient light. MSS is a portable skin analysis device, and robust to normal luminous conditions. However, it can analyze only a small region (<1 cm^2) at a time and hardly detects highly enlarged pores.

The aim of this study was to develop an image processing based facial pore analysis system which can automatically detect various sizes of pores and extract some features for analyzing the extent of pore widening. The system is then evaluated by comparing with the

conventional analytic devices using clinical references.

Materials and Methods

Subjects

Fifty healthy Koreans (25 males and 25 females) participated in this study. All volunteers have no physical or dermatologic disorders except mild acne. The mean age of the male subjects is 28.8 ± 2.8 (range, 23–36 years) and that of the female subjects is 28.2 ± 5.2 (range, 22–41 years). The study was approved by the Institutional Review Board of Korea University Anam Hospital and all participants gave informed consent prior to the study.

Image and data acquisition

Before photographing, the subjects were asked not to wear any make-up. Also, they relaxed in a constant temperature (24°C) and humidity room (relative humidity of 55%). Then, high-resolution full-face photographs were taken by JANUS, which has a built-in 1/1.6 in. CMOS DSLR camera (10M pixels). Three clinical photographs (2592×3888 pixels, in JPEG format) were taken successively from prefixed angles (one upper frontal and two 45° lateral photos).

When the user-defined region of interest (ROI) is given, JANUS yields the pore analysis score ranged from 0 to 100 for each ROI. In general, it provides partial analysis of four facial regions: forehead, nose, and both frontal cheeks. Thus, we cropped 300×300 pixel images, the actual size of which are 2×2 cm^2, from forehead and nose regions of the frontal image and left cheek region of the lateral image. We obtained a total of 150 clinical images from 50 subjects with the three different facial regions. Furthermore, among the whole subjects, 20 participants who gave informed consent about additional experiment were photographed with MSS to acquire three more images for each person. The three imaging regions were almost similar to, but smaller than, the ROI of JANUS (see Fig. 1).

Visual assessment

The images were clinically evaluated on a 5-point scale with grades from 0 (no visible pore on skin) to 4 (conspicuous and large pores) by two expert dermatologists (see Fig. 2). To measure the blind inter-rater reliability between these two experts, the intra-class correlation coefficient (ICC) was calculated using the two-way mixed model of raters and their grading results (9). In general, the ICC value larger than 0.70 indicates good to excellent reliability, and 0.40–0.60 represents moderate reliability (10, 11). The inter-rater reliability of two visual assessment grades shows high ICC values (0.78–0.86) and the average value of these two grades was employed to further assess the performance of the proposed method. Demographic data of the subjects and their pore grading are summarized in Table 1.

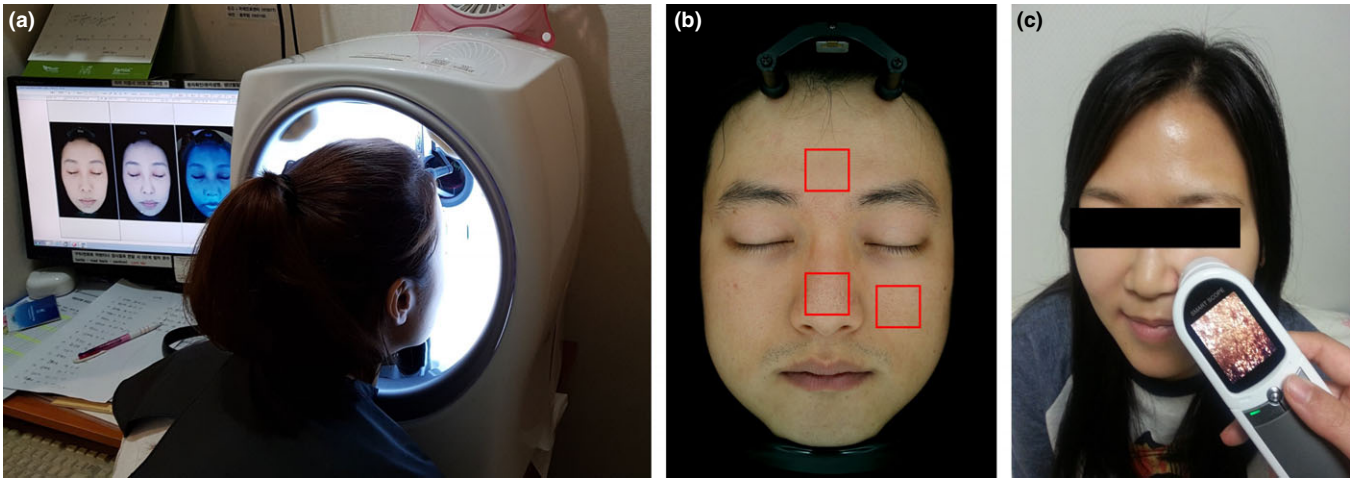

Fig. 1. Image acquisition. (a) Photographing using JANUS; (b) three ROIs (solid boxes) on forehead, nose, and left cheek area; (c) photographing using MSS. [Colour figure can be viewed at wileyonlinelibrary.com].

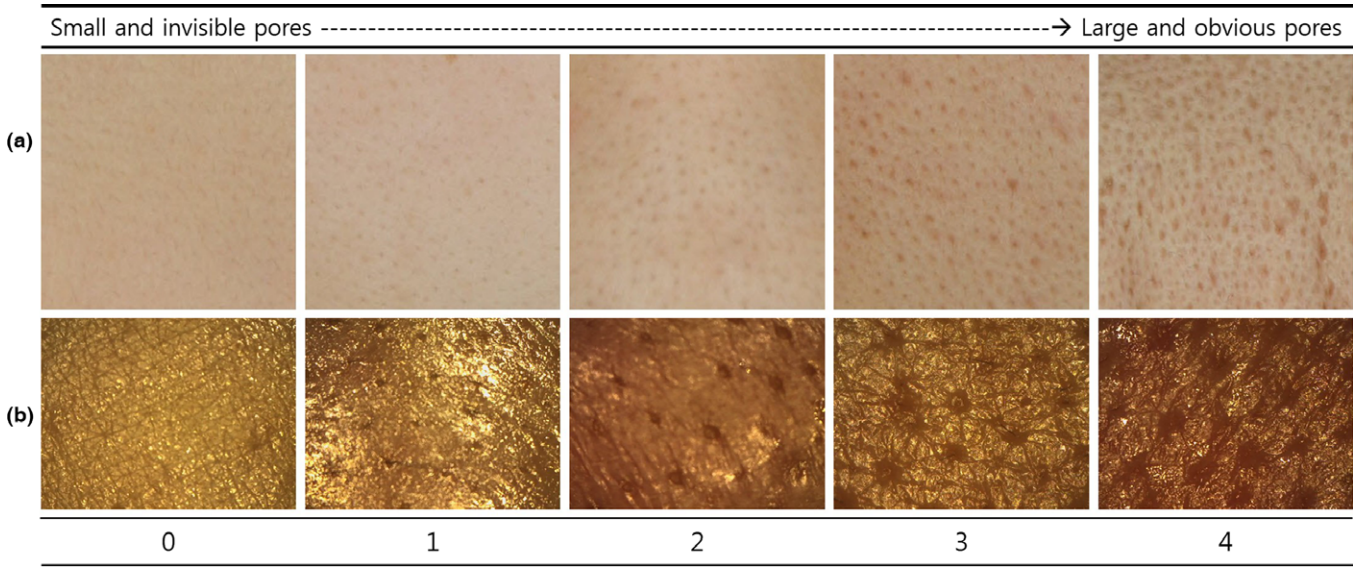

Fig. 2. Criteria of visual assessment for pore. (a) Representative images from JANUS and (b) those from MSS. [Colour figure can be viewed at wileyonlinelibrary.com].

TABLE 1. Age distribution and pore severity classification of the male and female subjects

Age	Total (n = 50)	Male (n = 25)	Female (n = 25)
20–24	9 (18%)	2 (8%)	7 (28%)
25–29	22 (44%)	12 (48%)	10 (40%)
30–34	13 (26%)	10 (40%)	3 (12%)
35–39	5 (10%)	1 (4%)	4 (16%)
40–44	1 (2%)	–	1 (4%)
Mean age		28.8 ± 2.8	28.2 ± 5.2

Pore grade (JANUS)	Total (n = 150)	Male (n = 75)	Female (n = 75)
Grade 0	11 (7.3%)	1 (1.3%)	10 (13.3%)
Grade 1	58 (38.7%)	27 (36.0%)	31 (41.3%)
Grade 2	56 (37.3%)	29 (38.7%)	27 (36.0%)
Grade 3	20 (13.3%)	14 (18.7%)	6 (8.0%)
Grade 4	5 (3.3%)	4 (5.3%)	1 (1.3%)

Pore grade (MSS)	Total (n = 60)	Male (n = 30)	Female (n = 30)
Grade 0	3 (5.0%)	0 (0.0%)	3 (10.0%)
Grade 1	12 (20.0%)	4 (13.3%)	8 (26.7%)
Grade 2	22 (36.7%)	12 (40.0%)	10 (33.3%)
Grade 3	14 (23.3%)	9 (30.0%)	5 (16.7%)
Grade 4	9 (15.0%)	5 (16.7%)	4 (13.3%)

Automatic pore detection and pore-related feature extraction

In this section, we introduce the proposed image processing method to detect various sized pores accurately and extract features to analyze the severity of pore enlargement. We first assume that the pores observed in the local skin images have the three properties as follows:

1 The pore region is relatively darker than its surroundings.
2 Pores appear to be blobs with similar sizes.
3 Pores are almost equally spaced.

The proposed method consists of four main stages: preprocessing, multi-scale pore detection, optimal scale selection, and feature extraction. In the preprocessing stage, the input RGB image is converted into grayscale, and then processed by local edge preserving (LEP) filter (12) to reduce the influence of non-uniform illumination. Based on the retinex theory (13), the LEP filter decomposes an input image into two layers, a piecewise smooth *base layer* containing larger scale variation in intensity and a *detail layer* which shows better details on the skin surface without illumination effect. Thus, we use the latter layer only, and histogram stretching (14) is performed on it in order to enhance the details (see Fig. 3a and b).

The 2nd property indicates that the local facial skin image has pores with a standard size value. Thus, we employ a multi-scale pore detection scheme which assumes the standard size of pores as multiple levels of area values and detects the pore blobs based on the relative darkness and the size similarity to the assumed area value for each scale.

According to the 1st property, the pore candidates are extracted using the luminance ratio (LR), the ratio of the intensity of center pixel to the average intensity of pixels in its scale-varying local neighborhood. The pixels with lower LR than a certain threshold T_R are extracted

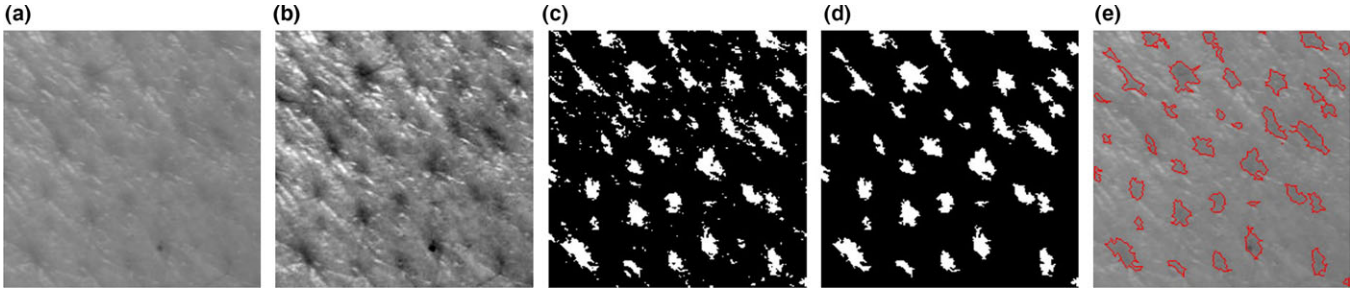

Fig. 3. Illustration of the pore detection process. (a) The input image in grayscale, (b) the luminance-free image after preprocessing stage, (c) the pore candidates (white blobs), (d) the extracted pores using the score function, and (e) the borders of the extracted pores over the input facial image. [Colour figure can be viewed at wileyonlinelibrary.com].

and grouped into pore candidate blobs by connected component labeling (15) based on eight-connectivity. When the candidate blob is larger than twice the assumed area, darker pixels in the large blob are additionally extracted and grouped into new smaller blobs (see Fig. 3c).

To determine whether a candidate blob is a pore or not, each blob is evaluated using a score function formulated based on two factors: the relative darkness and the area similarity to the assumed area of each scale. The score function gives a high score to the candidate blob having a low average LR and an area value similar to the assumed one. As a result, the blob whose score is higher than a threshold T_S is detected as a real pore (see Fig. 3d and e). The pore blobs are detected for each level of the multi-scale detection scheme by three consecutive processes: LR computation, candidate blob search, and real pore extraction using the score function.

Among the detection results obtained by the multi-scale pore detection process, we select the most appropriate scale and its corresponding detection result based on the 3rd property of pores. The dots in the ground truth (Fig. 4b) and the detection results (Fig. 4c–e) indicate the center points of real pores and the detected ones, respectively. The result with most equally spaced pores (Fig. 4e) exhibits the most similar pore distribution to the ground truth, coinciding with the 3rd property.

To select the result with equally spaced pores, we measure the distance between pores using Delaunay triangulation (DT) (16). The black lines in Fig. 4c–e show the result of DT applied to the centers of detected pores, and each side length of triangles corresponds to the distance between two pores. The uniformity of the side lengths is measured by computing the coefficient of variation (CV) (17) for each scale. The lower CV value indicates that its corresponding pore detection result has more evenly spaced pores. In this example, the third scale (Fig. 4e) has the lowest CV value, and therefore its corresponding result is automatically selected.

Finally, we extract pore-related features such as the number of pores, total pore area, average size, and average depth from the final pore detection result. The former three features can be obtained simply by counting the number of pixels belonging to the pore blobs and dividing the total area by the number of pores. The average depth of pore is defined as the ratio between representative intensity value of pore region and that of non-pore region.

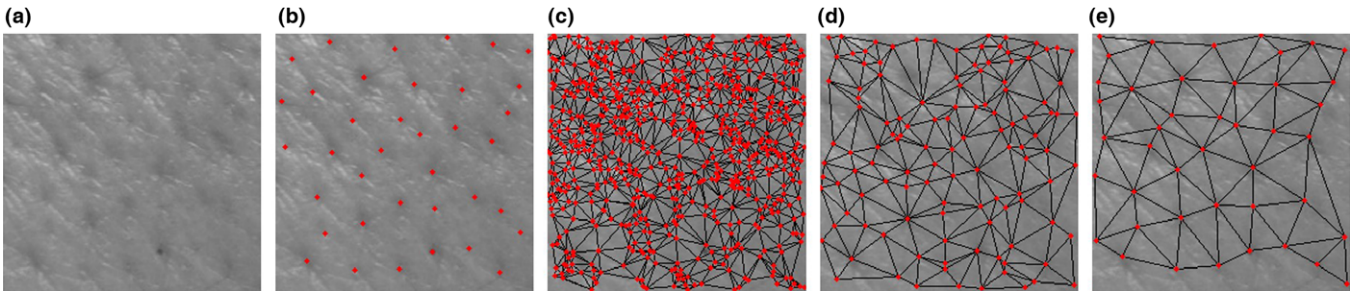

Fig. 4. (a) Input image, (b) the ground truth pores marked with dots, and the result of Delaunay triangulation based on the center points of detected pores for (c) 1st, (d) 2nd, and (e) 3rd scale. The CV values for the three scales are 0.460, 0.395, and 0.277, respectively. [Colour figure can be viewed at wileyonlinelibrary.com].

Statistical analysis

Correlation analysis between the visual grading and each pore-related feature was performed, and then the final pore score was calculated based on the analysis results. Furthermore, we utilized the Spearman's correlation coefficient, ρ, to measure the correlation between the visual assessment scores (ordinal categorical variable) and three objective pore scores (continuous variables) obtained from JANUS, MSS, and the proposed system. To interpret the correlation coefficient, we used Colton's recommendation (18) of ρ = 0.25–0.50 to be fair, ρ = 0.50–0.75 to be moderate to good, and ρ > 0.75 to be very good to excellent. All statistical analyses were conducted using statistical software (SPSS Statistics 23.0; SPSS Inc., Chicago, IL, USA) and a $P < 0.001$ is considered statistically significant.

Results

Relation between clinical score and extracted features

The correlations between the visual grading and the extracted pore-related features were analyzed using the facial skin images taken by JANUS and MSS. Although there is no gold standard for visual grading, the high inter-rater reliability indicates that the clinical score can be a valid measure for evaluating the extent of pore enlargement. The correlation analysis was performed separately for men and women, and the detailed results associated with JANUS images are shown in Fig. 5 and Table 2. Note that, for both sexes, the clinical score is highly correlated ($\rho > 0.767$, $P < 0.001$) with the number of the large pores, moderately correlated ($\rho > 0.668$, $P < 0.001$) with the total area, the average size, and the average depth whereas the number of small pores is negatively correlated with the clinical scores. Unlike other features, the number of medium pores does not show any significant correlation.

Figure 6 and Table 2 show that the similar trends can be observed for the images taken by MSS. The number of large pores, the total area, and the average size are highly correlated for both sexes, except for the total pore area in women; besides, there is a negative relationship for the number of small pores and no correlation for that of medium pores. The only noticeable difference is that the average depth, which has strong correlation in JANUS images, appears to have very weak correlation in MSS images.

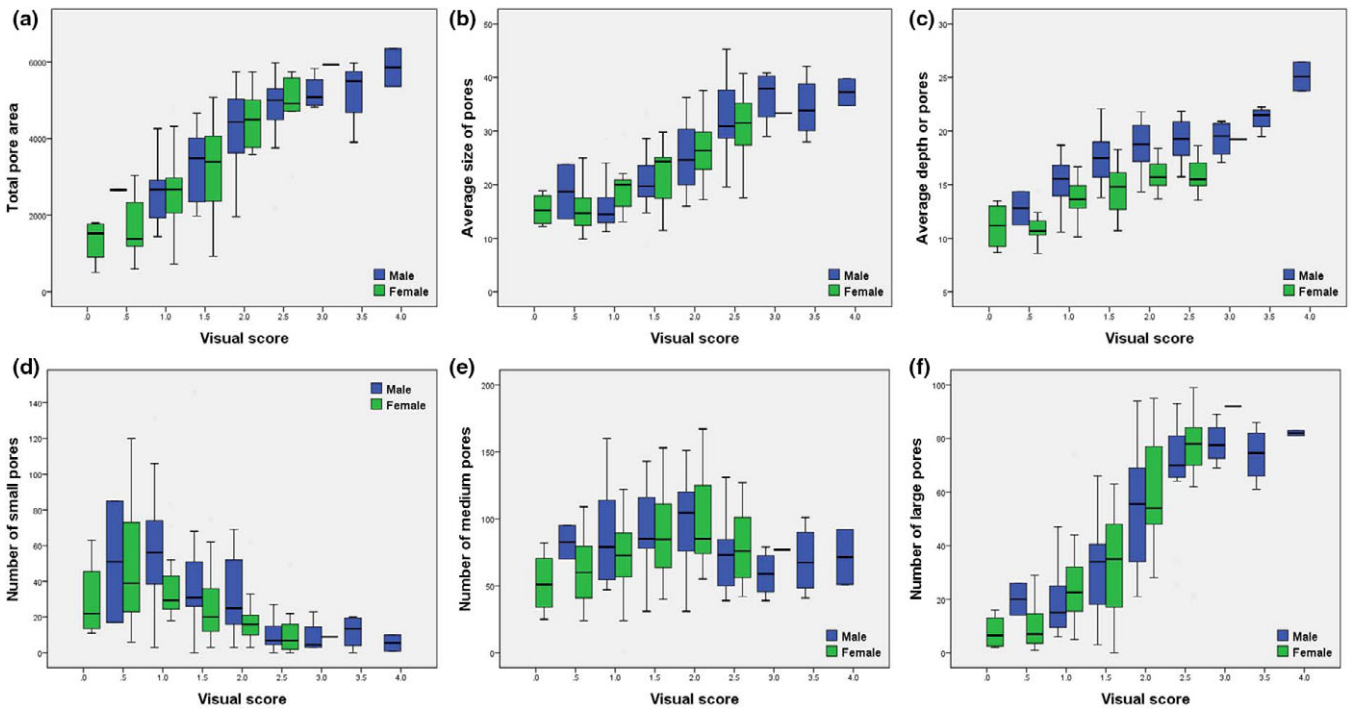

Fig. 5. Boxplots of clinical scores vs. pore-related features measured from JANUS images, separately for men and women. The average clinical scores are shown on the x-axis and the pore-related features on the y-axis. The band in the box represent the median, with the bottom and top parts the first and third quartile. Each boxplot represents the relationship between the clinical reference and the pore-related features: (a) total pore area; (b) average pore size; (c) average pore depth; the number of (d) small, (e) medium, and (f) large pores. [Colour figure can be viewed at wileyonlinelibrary.com].

TABLE 2. Correlation between visual assessment and pore-related features

Imaging device	Feature	Male (n = 25)		Female (n = 25)	
		Mean ± SD	ρ	Mean ± SD	ρ
JANUS	Total area	3848.62 ± 1366.89	0.717*	3261.48 ± 1449.86	0.791*
	Average size	24.63 ± 9.17	0.770*	22.13 ± 7.08	0.696*
	Average depth	17.89 ± 3.06	0.668*	14.14 ± 2.48	0.678*
	Number of pores				
	S < 10	33.15 ± 30.89	−0.663*	28.51 ± 24.08	−0.482*
	10 < S < 50	84.45 ± 31.41	−0.244	78.97 ± 32.12	0.306**
	50 < S	45.13 ± 27.79	0.786*	37.39 ± 27.45	0.767*
MSS	Total area	23,459.43 ± 6889.86	0.683*	19,923.90 ± 4969.16	0.243
	Average size	856.03 ± 380.20	0.703*	629.95 ± 395.33	0.786*
	Average depth	17.44 ± 4.19	0.124	16.32 ± 4.26	0.319
	Number of pores				
	S < 500	20.17 ± 31.93	−0.573**	58.6 ± 79.46	−0.719*
	500 < S < 1000	7.50 ± 3.98	0.163	4.80 ± 3.70	0.492**
	1000 < S	7.20 ± 4.58	0.624*	5.33 ± 4.48	0.762*

SD, standard deviation; ρ, Spearman's correlation coefficient; S, Size of each pore blob.
*P < 0.001; **P < 0.01.

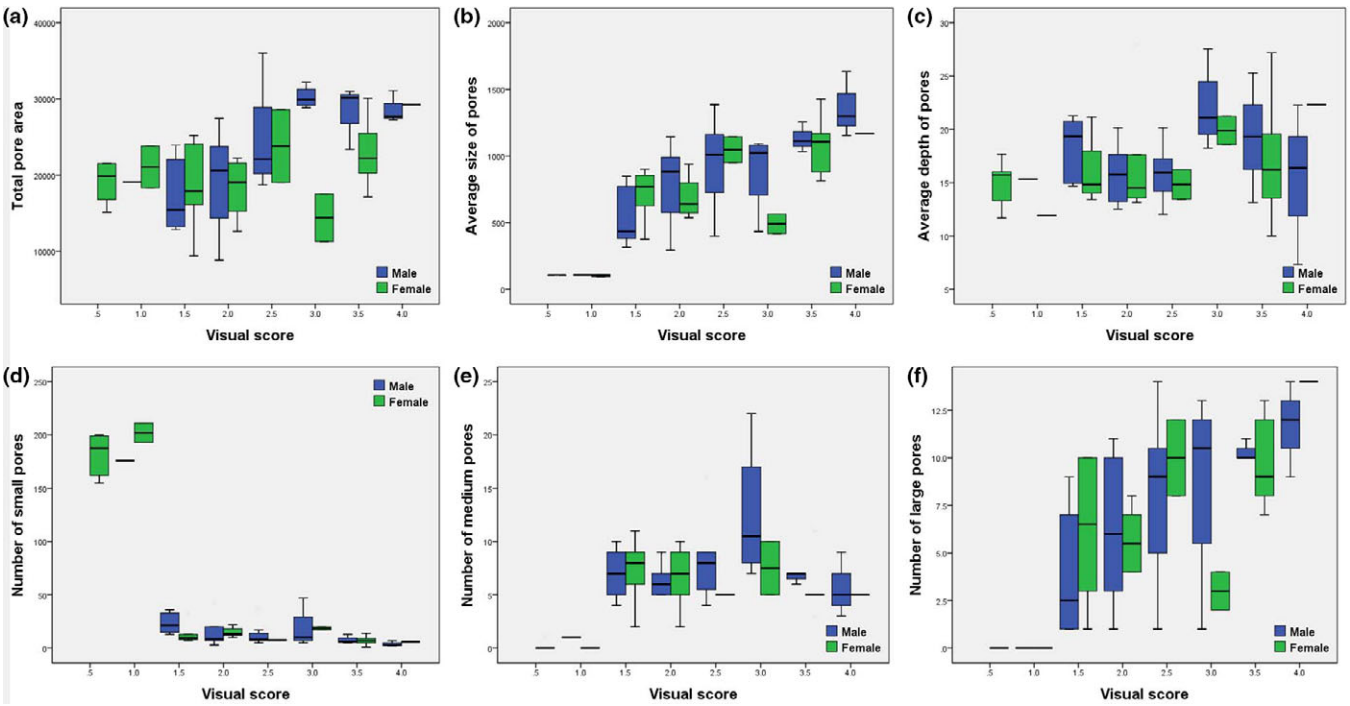

Fig. 6. Boxplots of clinical scores vs. pore-related features measured from MSS images, separately for men and women. Each boxplot represents the relationship between the clinical reference and the pore-related features: (a) total pore area; (b) average pore size; (c) average pore depth; the number of (d) small, (e) medium, and (f) large pores. [Colour figure can be viewed at wileyonlinelibrary.com].

We formulated the final pore score function reflecting the aforementioned results of correlation analysis. More specifically, the final score, [0,100], is proportional to the number of large pores and the average size, but inversely proportional to the number of small pores in the skin images.

Comparative evaluation on a commercialized analytic apparatus

To verify the effectiveness of our pore analysis system, we computed the correlation coefficient between the clinical scores and three objective scores obtained by JANUS, MSS, and the proposed system. There is relatively low

correlation ($\rho = 0.329$, $P < 0.001$) between the JANUS score and the visual grading since its analytic software only uses the total pore area value and the intensity to calculate the score. On the other hand, our system, which additionally exploits more features such as the number of pores depending on their size and the average depth, shows a significant correlation ($\rho = 0.818$, $P < 0.001$) to the clinical score (see Fig. 8a and Table 3).

TABLE 3. Spearman's correlation coefficient of pore analysis methods

Imaging device	ρ_{Conv}	$\rho_{Proposed}$
JANUS	0.329*	0.818*
MSS	0.569*	0.765*

ρ_{Conv} Correlation coefficient between the clinical scores and the pore score calculated by conventional analytic software; $\rho_{Proposed}$: Correlation coefficient between the clinical scores and the pore score calculated by the proposed analysis system.
*$P < 0.001$.

Unlike JANUS, MSS provides the detection results as well as the pore score. Thus, we were able to compare the detection results obtained by MSS software and the proposed one. Figure 7 illustrates some examples of the input and detected images, in which pores are enclosed

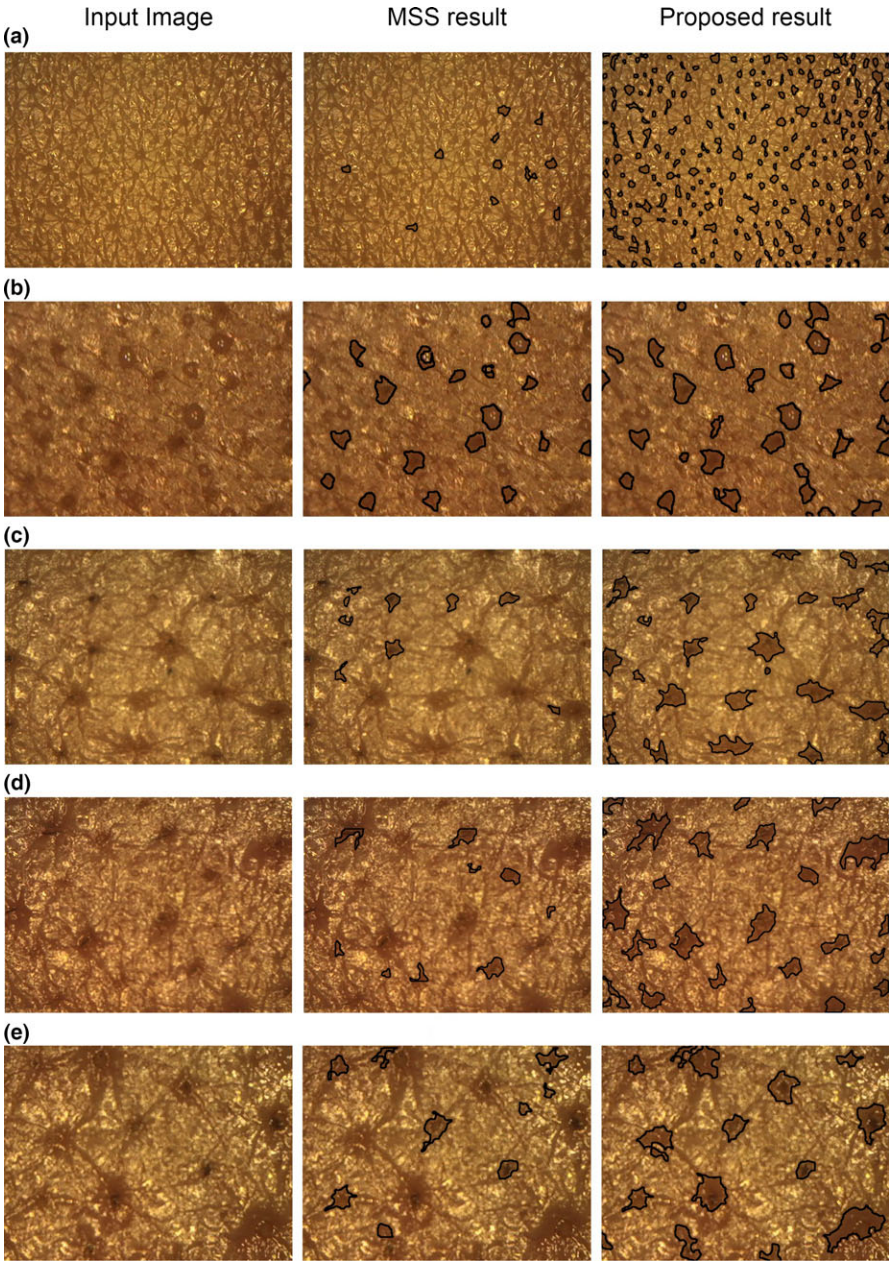

Fig. 7. Input images and the corresponding pore detection results obtained using the conventional apparatus, MSS, and the proposed method (from a–e, the facial pores getting larger). [Colour figure can be viewed at wileyonlinelibrary.com].

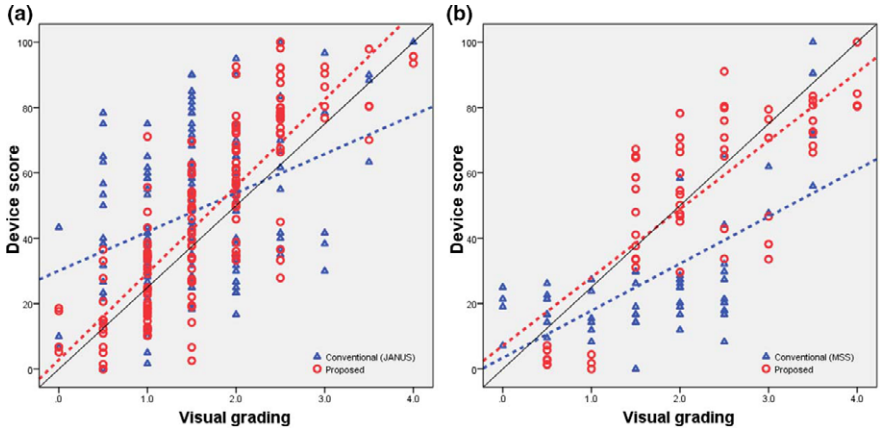

Fig. 8. Scatter plot of clinical scores vs. objective score of pore widening calculated by the inherent software program of conventional devices (triangles) and the proposed method (circles). (a) Comparison with JANUS. (b) Comparison with MSS. The more the data points agree with the black solid line (slope of 1), the higher correlated with the visual grading. [Colour figure can be viewed at wileyonlinelibrary.com].

with the black boundary lines. The proposed method detects various sizes of pores accurately whereas MSS often fails to extract not only fine pores (Fig. 7a) but also some highly enlarged ones (Fig. 7c–e). Figure 8b and Table 3 show that our analysis result is more strongly correlated ($\rho = 0.765$, $P < 0.001$) with the clinical grading than the MSS result ($\rho = 0.569$, $P < 0.001$).

Conclusion

The proposed facial pore-analyzing system automatically detects various sizes of pores and calculates the pore score indicating the extent of pore enlargement by exploiting the relationship between the pore-related features and the clinical reference. The pore score calculated by the proposed method has the stronger correlation with the clinical grading as compared with those obtained by the conventional analytic apparatuses. In conclusion, the proposed method is not only highly effective in quantitative measurement on the degree of pore widening, but also suitable for objective assessment of treatment modalities for pore tightening.

References

1. Pie′rard GE, Elsner P, Marks R, Masson P, Paye M. EEMCO guidance for the efficacy assessment of antiperspirants and deodorants. Skin Pharmacol Appl Skin Physiol 2003; 16: 324–342.
2. Piérard GE, Piérard-Franchimont C, Marks R, Paye M, Rogiers V. EEMCO guidance for the in vivo assessment of skin greasiness. Skin Pharmacol Appl Skin Physiol 2000; 13: 372–389.
3. Lee SY, Lee S, Cho HK. The insight on skin pores with cosmetic concern in Korean women. Korean Journal of Dermatology 2012; 50: 510–515.
4. Kang S, Krueger GG, Tanghetti EA, Lew-Kaya D, Sefton J, Walker PS, Gibson JR. A multicenter, randomized, double-blind trial of tazarotene 0.1% cream in the treatment of photodamage. J Am Acad Dermatol 2005; 52: 268–274.
5. Kakudo N, Kushida S, Tanaka N, Minakata T, Suzuki K, Kusumoto K. A novel method to measure conspicuous facial pores using computer analysis of digital-camera-captured images: the effect of glycolic acid chemical peeling. Skin Res Technol 2011; 17: 427–433.
6. Saedi N, Petrell K, Arndt K, Dover J. Evaluating facial pores and skin texture after low-energy nonablative fractional 1440-nm laser treatments. J Am Acad Dermatol 2013; 68: 113–118.
7. Campolmi P, Bonan P, Cannarozzo G, Bruscino N, Moretti S. Efficacy and safety evaluation of an innovative CO_2 laser/radiofrequency device in dermatology. J Eur Acad Dermatol Venereol 2013; 27: 1481–1490.
8. Kim JE, Lee HW, Kim JK, Moon SH, Ko JY, Lee MW, Chang SE. Objective evaluation of the clinical efficacy of fractional radiofrequency treatment for acne scars and enlarged pores in Asian skin. Dermatol Surg 2014; 40: 988–995.
9. McGraw KO, Wong SP. Forming inferences about some intraclass correlation coefficients. Psychol Methods 1996; 1: 30–46.
10. Nunnally JC, Bernstein IH. Psychometric theory, 3rd edn. New York: McGraw-Hill Inc., 1994.
11. Terwee CB, Bot SD, de Boer MR, van der Windt DA, Knol DL, Dekker J, Bouter LM, de Vet HC. Quality criteria were proposed for measurement properties of health status questionnaires. J Clin Epidemiol 2007; 60: 34–42.
12. Gu B, Li W, Zhu M, Wang M. Local edge-preserving multiscale decomposition for high dynamic range image tone mapping. IEEE Trans Image Process 2013; 22: 70–79.
13. Land EH. The retinex theory of color vision. Sci Am 1977; 237: 108–128.
14. Vernon D. Fundamentals of digital image processing. In: Machine

vision - Automated visual inspection and robot vision. Englewood Cliffs, NJ: Prentice Hall; 1991: 46–49.
15. Acharya T, Ray AK. Dynamic scene analysis: moving object detection and tracking. Image processing: principles and applications. Hoboken, NJ: Wiley; 2005: 311–312.
16. Berg MD Cheong O, Kreveld M, Overmars M. Delaunay triangulations. In: Computational geometry: algorithms and applications. New York: Springer-Verlag; 2008: 191–218.
17. Brown C. Coefficient of variation. In: Applied multivariate statistics in geohydrology and related sciences. New York: Springer-Verlag; 1998: 155–157.
18. Colton T. Statistics in medicine. Boston, MA: Little, Brown and Company, 1974: 211.

Address:
Sung Jea Ko
Department of Electrical Engineering
Korea University
145, Anam-ro, Seongbuk-gu
Seoul 02841
Korea
Tel: +82-2-3290-3228
Fax: +82-2-925-5883
e-mail: sjko@korea.ac.kr